Imaging Spectrum of Double-Outlet Right Ventricle on Multislice Computed Tomography

Sarv Priya, MD,* Prashant Nagpal, MD,* Arun Sharma, MD,†
Niraj N. Pandey, MD, DNB,† and Priya Jagia, MD†

Abstract: Double-outlet right ventricle is a complex congenital heart disease that encompasses various common and rare subtypes. Surgical management of these patients needs to be individualized owing to extremely variable morphology and hemodynamics. Imaging plays a crucial role in determination and characterization of outflow tract morphology. The assessment of ventricular septal defect routability with identification of associated anomalies has therapeutic implications in these patients. Multislice computed tomography with advanced 3-dimensional postprocessing techniques and dose-reduction strategies is invaluable in defining the anatomy and morphology of double-outlet right ventricle with simultaneous assessment of associated anomalies.

Key Words: double-outlet right ventricle, ventricular septal defect, routability, conus, computed tomography, volume rendered, 3-dimensional, virtual reality

(*J Thorac Imaging* 2019;34:W89–W99)

Double-outlet right ventricle (DORV) is a complex congenital heart disease, wherein both the pulmonary artery and aorta are committed either > 50% or completely to the right ventricle (RV). Echocardiography, although highly operator dependent, often constitutes the first-line of diagnostic imaging. Catheter angiography, formerly considered the reference standard of diagnosis, is an invasive procedure with high radiation exposure and inherent risk of catheter-related complications.[1] Magnetic resonance imaging (MRI) is a promising imaging tool in the preoperative as well as postoperative assessment because of lack of associated radiation risks and the availability of accurate functional assessment. However, it has several inherent disadvantages including long acquisition times, need for sedation or general anesthesia, poor spatial resolution, limited availability, and higher cost.[2] The need for high spatial resolution and requirement of motion artefact–free images remains a challenge, especially in small children.

Current-generation computed tomography (CT) scanners can provide excellent image quality with high spatial and temporal resolution in these cases. Moreover, recent technical advancements including use of wider detectors, faster gantry rotation times, and high-pitch scanning have resulted in reduction of the scanning time as well as radiation dose in this subset of pediatric patients.[3] Moreover, CT generally requires no sedation, owing to shorter scan duration, and thus allows for detailed evaluation of extracardiac abnormalities as well. Use of prospective ECG gating in pediatric patients with regular and low heart rate is associated with even further reduction in radiation dose. The CT data set can also be used in 3D printing, which can be useful in planning and predicting successful surgical outcome in complex cases. In this pictorial essay, we present the imaging spectrum of DORV and key anatomic parameters that affect surgical planning by using multidetector CT data.

IMAGING PROTOCOL

Imaging was performed on a dual-source 384 (2×192)-slice CT machine (Somatom Force; Siemens, Erlangen, Germany). Scanning was performed with care dose 4D and
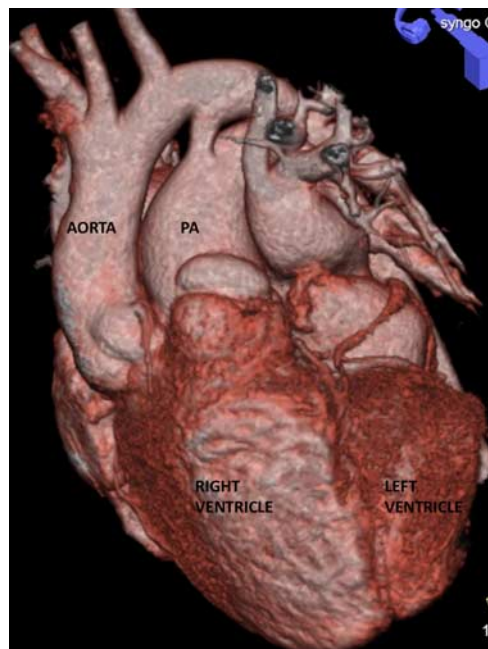
DOI: 10.1097/RTI.0000000000000396

FIGURE 1. Double-outlet right ventricle. Three-dimensional volume-rendered images of CT angiography show both aorta and pulmonary artery arising entirely (200% rule) from the right ventricle. PA indicates pulmonary artery.
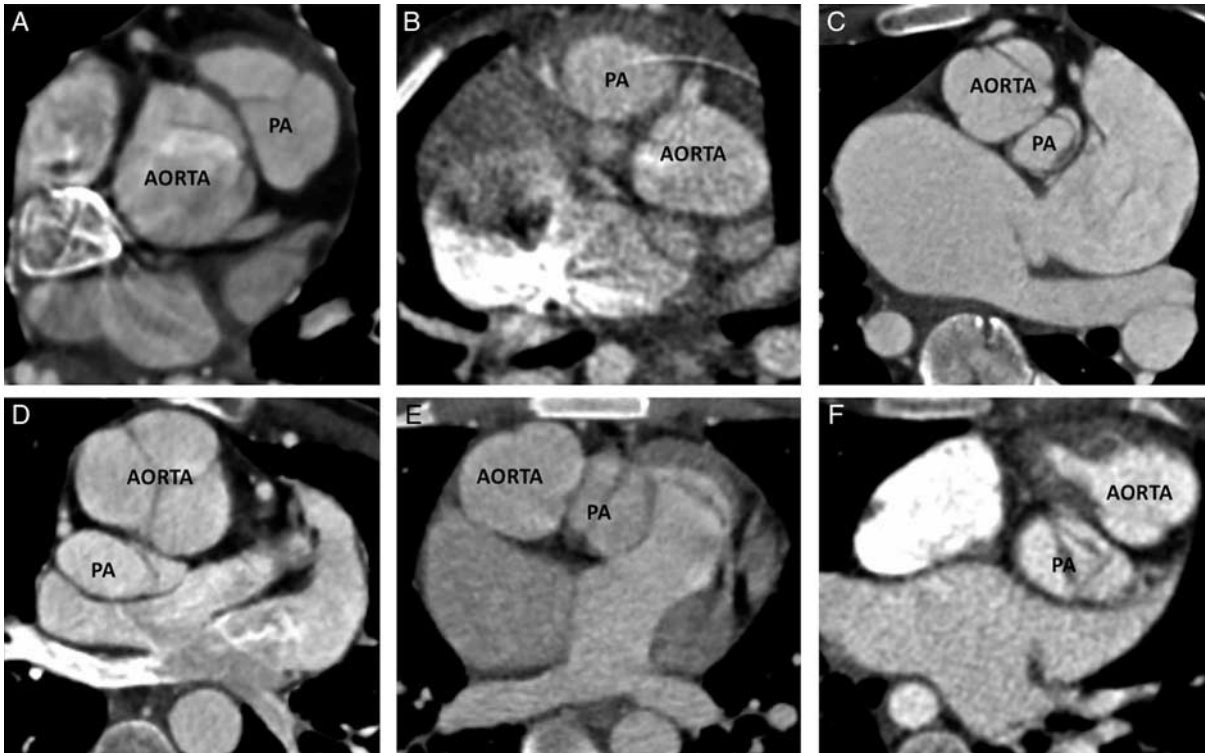
FIGURE 2. Malposition of great arteries. Axial CT angiography images in different patients depicting relationship of great arteries. A, The aorta is seen posterior and to the right of the pulmonary artery (normal relationship). B, The aorta is posterior and to the left of the pulmonary artery. C, Dextroposed aorta. D, The aorta directly anterior to the pulmonary artery. E, Side-by-side great arteries. F, Levoposed aorta. PA indicates pulmonary artery.

using scanner-selected kV and mA. Prospective or retrospective scanning with ECG-gated dose modulation was performed (maximum dose range was from 70% to 80% or 30% to 80% of the cardiac cycle if coronary evaluation was also required). Manual bolus tracking was performed, and the scan was triggered after visualization of contrast in the descending aorta. Delayed non–ECG-gated imaging was performed in patients who required venous evaluation as well. The intravenous line was preferred in the right arm. Nonionic iodinated contrast (Omnipaque, 350 mgI/ml or Isovue, 370 mgI/ml) was given intravenously by dual-head power injector followed by saline bolus at a similar rate. The

rate of injection was dependent on IV gauge (20 to 24), but, in the majority of patients, the rate was 1.5 to 2.5 mL/s.

Classification

DORV, as the name suggests, is characterized by ventriculoarterial discordance, wherein the whole of one great artery and 50% or more of the other (150% rule) or both great arteries completely (200% rule) (Fig. 1, Supplemental Video 1, Supplemental Digital Content 1, http://links.lww.com/JTI/A115) arise from the RV.[4] Therefore, the only pathway by which the left ventricle (LV) empties itself is a ventricular septal defect (VSD). CT angiography, in
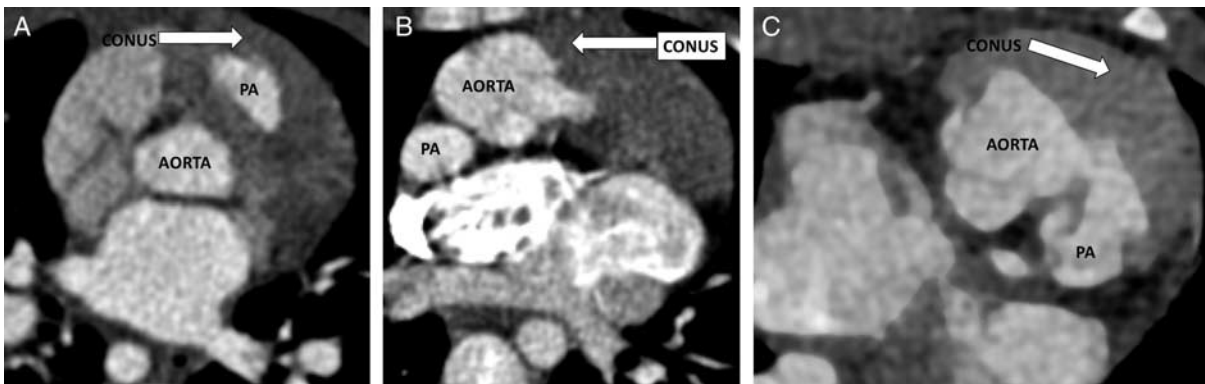

FIGURE 3. Conus (infundibulum). Axial CT angiography images showing the position of the conus. Subpulmonary conus (A), subaortic conus (B), double conus (muscle bundle beneath both semilunar valves) (C).
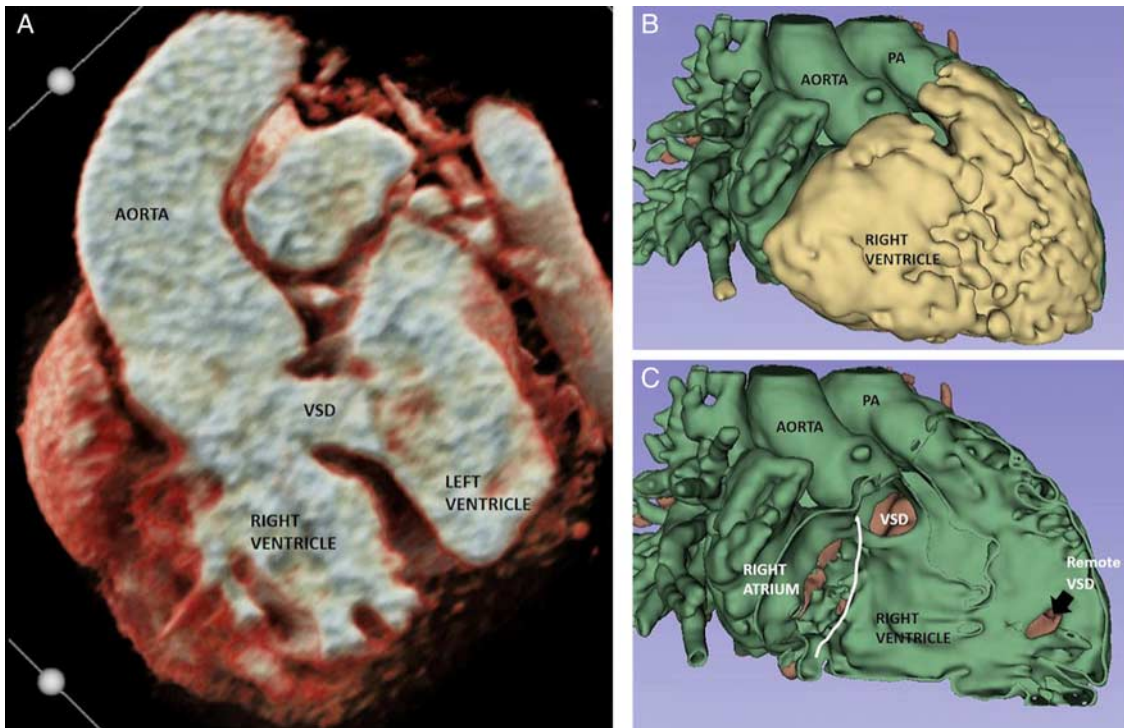
FIGURE 4. Subaortic VSD. A, Front cut view of volume-rendered image showing subaortic location of VSD. B, Volume-rendered image showing double-outlet right ventricle before removing part of the right ventricle (yellow color). C, The front cut plane (endocardial representation after removing right ventricle surface) of the volume-rendered model shows location of the VSD (as seen from the right ventricle) beneath the aortic valve and the abutting upper one third of the tricuspid valve. Through the VSD, the left ventricle is seen (brown color). The white line represents tricuspid valve plane. PA indicates pulmonary artery.
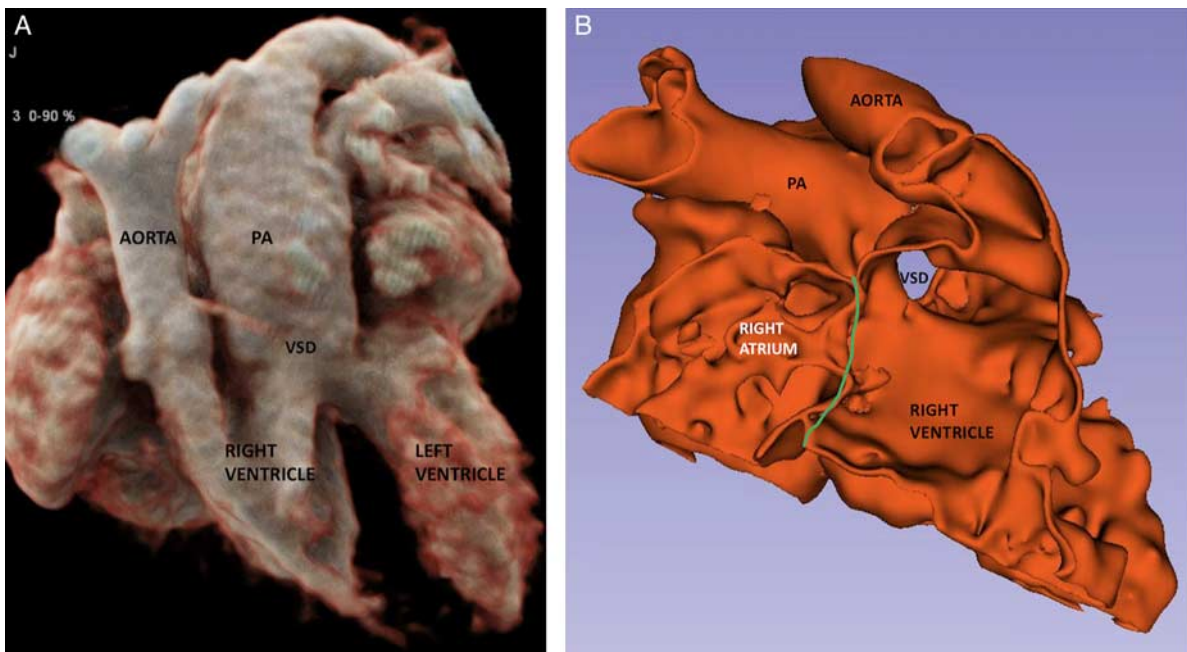

FIGURE 5. Subpulmonary VSD. A, Volume-rendered image showing subpulmonary location of VSD. B. The front cut plane (endocardial representation after removing right ventricle surface) of the volume-rendered model shows the location of the VSD (as seen from the right ventricle) beneath the pulmonary valve. The green line represents tricuspid valve plane. PA indicates pulmonary artery.
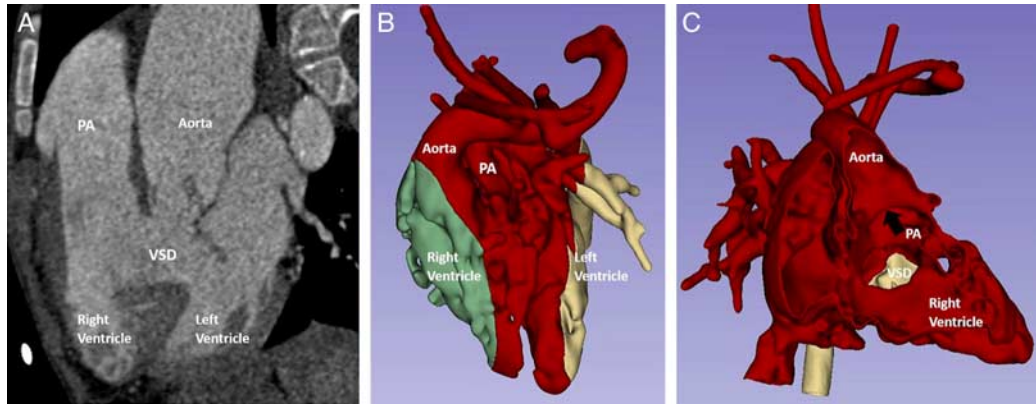
FIGURE 6. Doubly committed and remote VSD. A, Reformatted coronal CT angiography image with doubly committed VSD (VSD in relation to both semilunar valves). B, Volume-rendered model shows DORV before removing part of the right ventricle (green color). C, The front cut plane (endocardial representation after removing right ventricle surface) of the volume-rendered model shows the remote location of the VSD (as seen from the right ventricle), away from the semilunar valve and toward the right ventricle inlet. Through the VSD, the left ventricle is seen (yellow color). PA indicates pulmonary artery.

FIGURE 7. Routability. Multiplanar reformatted CT angiography oblique image shows the path of the LV to aorta baffle in a patient with subaortic VSD. PA indicates pulmonary artery

addition to demonstrating the anomalous ventriculoarterial connection, provides key information with regard to routability of the VSD and presence of other associated malformations that influence preoperative planning.[5] The classification of DORV is primarily based on the location of VSD and the presence/absence of pulmonary stenosis (PS), with the most common subtypes of DORV being as follows:

  (i) Tetrology of Fallot-type variant (subaortic VSD with PS).
 (ii) Transposition of great arteries-type variant (subpulmonary VSD without PS): Taussig-Bing anomaly.
(iii) VSD-type variant (subaortic VSD without PS).
(iv) Univentricular heart–type variant (DORV with mitral atresia, unbalanced atrioventricular canal, or presence of severe hypoplasia of one of the ventricular sinuses).[6,7]

VSD location with respect to the aortic and pulmonary valves significantly affects the physiology and influences the surgical management in cases of DORV. The VSD may be as follows:
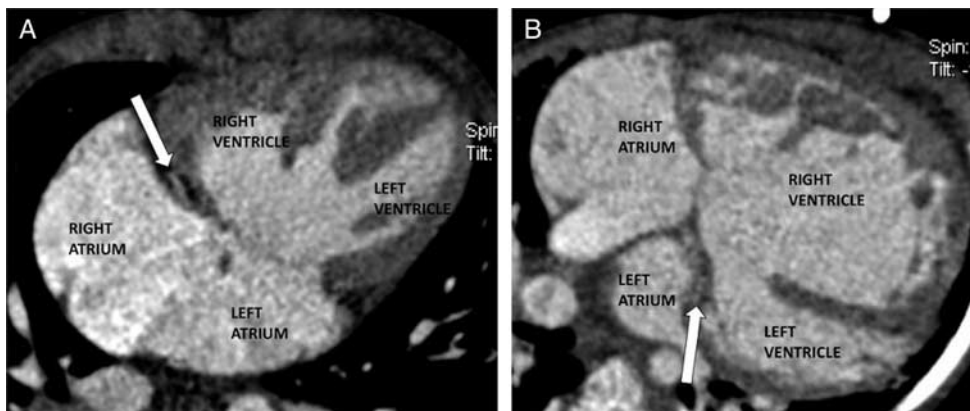

FIGURE 8. Associated atrioventricular valve anomalies. Axial CT angiography images in 2 different patients showing atrioventricular valve morphology. A, Tricuspid atresia (atretic tricuspid valve indicated by arrow). B, Mitral atresia (atretic mitral valve indicated by arrow): left ventricular end-diastolic volume was 18 mL.
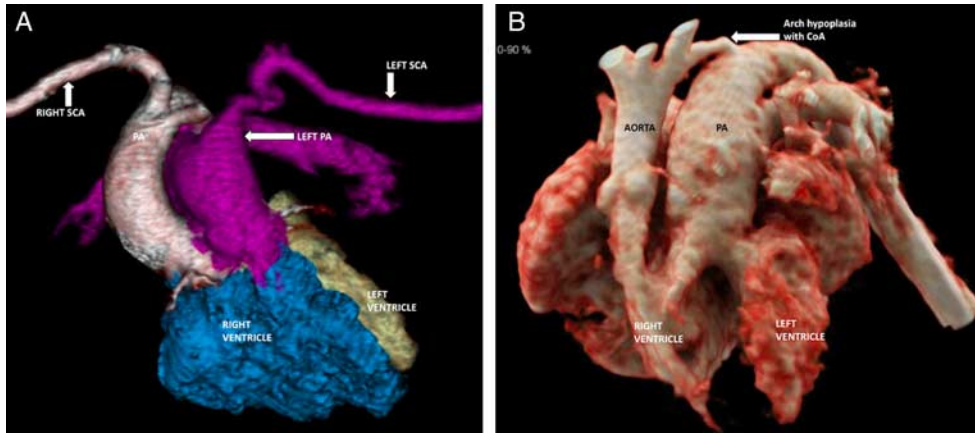
FIGURE 9. Associated aortic variations and anomalies. A, Volume-rendered image in a patient with double-outlet right ventricle shows origin of the left subclavian artery from the left pulmonary artery. B, Cinematic volume-rendered image in another patient with double-outlet right ventricle shows arch hypoplasia with coarctation of the aorta. CoA indicates coarctation of aorta; PA, pulmonary artery; SCA, subclavian artery.
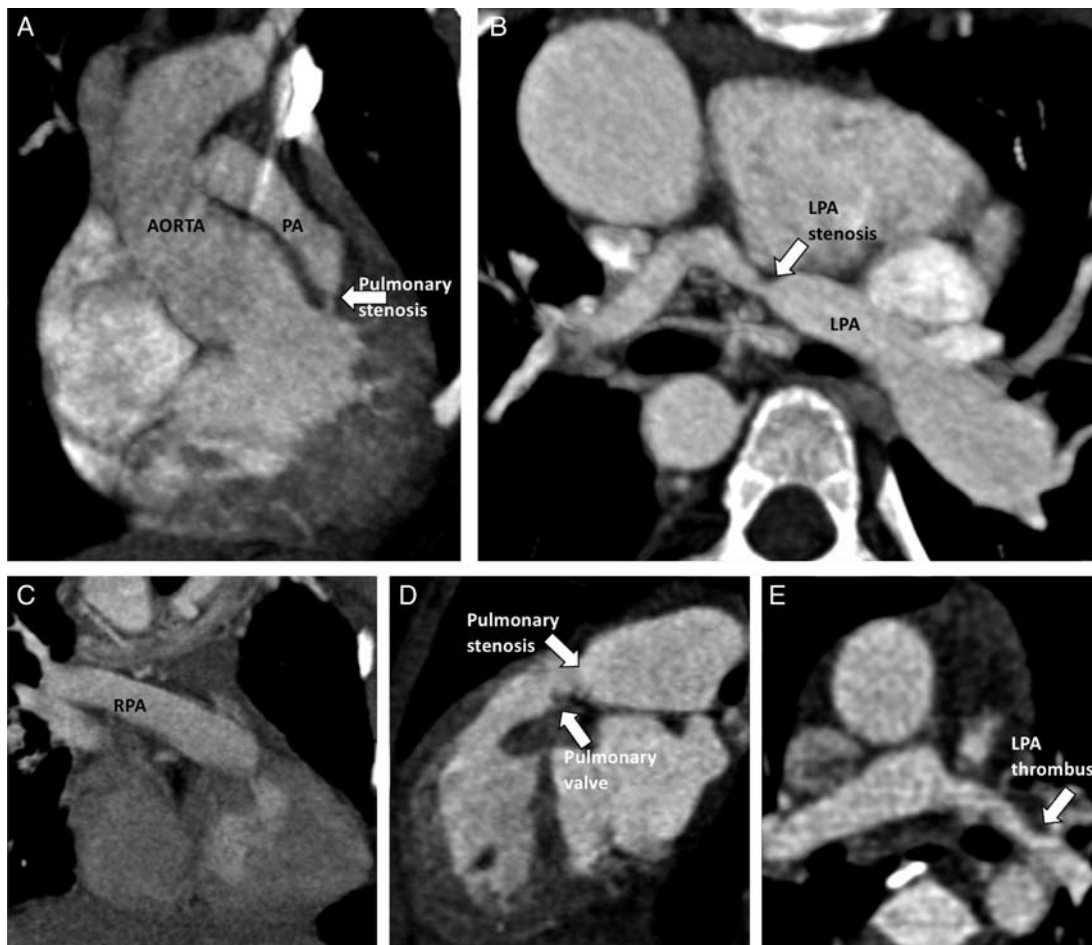
FIGURE 10. Associated pulmonary arterial abnormalities. A, Reformatted coronal CT angiography (CTA) image shows severe infundibular pulmonary stenosis. B, Axial CTA image in a patient shows left pulmonary artery stenosis with poststenotic dilatation. C, Reformatted coronal CTA image shows nonvisualization of the left pulmonary artery (LPA atresia): only the right pulmonary artery is seen. D, Reformatted sagittal CTA image shows supravalvular pulmonary stenosis. E, Axial CTA image in a patient shows eccentric left pulmonary artery thrombus. LPA indicates left pulmonary artery; RPA, right pulmonary artery; PA, pulmonary artery.

FIGURE 11. Associated anomalies of systemic venous drainage. A, Coronal reformatted CT angiography (CTA) images show bilateral superior vena cava. B, Axial abdominal CTA image with duplicate inferior vena cava. C, Multiplanar coronal reformatted CTA image shows retroaortic course of left innominate vein. D, Coronal reformatted CTA image shows direct drainage of hepatic veins into the left atria. IVC indicates inferior vena cava; SVC: superior vena cava.

 (v) subaortic;
 (vi) subpulmonary;
 (vii) noncommitted or remote; and
(viii) doubly committed in relation to the semilunar valves.[7]

Approach to Diagnosis on Imaging

The major points of concern in the imaging assessment of these cases include determining the great vessel relationship, identification and categorization of conus, assessing the location and routabilty of the VSD along with identification of associated anomalies, which can have an impact on the management.

Relationship of Great Arteries

DORV can be associated with various arrangements in the orientation of the great arteries.[6] They may be in a side by side relationship or can have a normal relationship in which the aorta is posterior, inferior, and to the right of the pulmonary artery, or can be malposed with the aorta being directly anterior or posterior and to the left of the pulmonary artery. The aorta can also be dextroposed or levoposed (Fig. 2). In fact, it is the rotation of the great arteries driven by the conal development that is responsible for the diverse spectrum of DORV.

Conus

There are various conal morphologies in between the spectrum of predominantly subaortic and subpulmonary conus (Fig. 3).[7–9] These variations impact the physiology and should be approached with an individualized management plan.
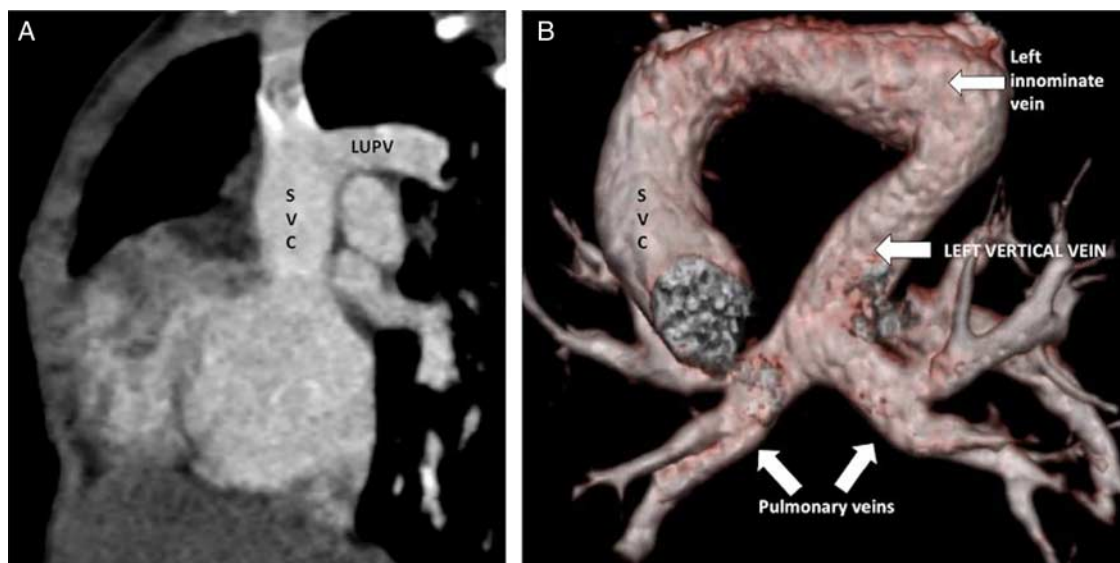
FIGURE 12. Associated anomalies of pulmonary venous drainage. A, Reformatted sagittal CT angiography image shows drainage of the left upper pulmonary vein into the superior vena cava (partial anomalous pulmonary venous connection). B, Volume-rendered image showing total anomalous pulmonary venous connection: all pulmonary veins drain into the left innominate vein via the left vertical vein. LUPV indicates left upper lobe pulmonary vein; SVC: superior vena cava.

In the most commonly observed classic tetralogy of Fallot-type DORV, there is a near-normal length of the conus beneath the pulmonary valve and minimal conus beneath the aortic valve. This results in aortomitral discontinuity, and the pulmonary valve assumes an anterior and superior position.

Similarly, the second most common DORV variant has the conus mostly under the aortic valve along with a small amount of conus under the pulmonary valve, which results in loss of pulmonary-mitral continuity. This form is physiologically similar to transposition of the great arteries.

Between the classic tetralogy type and the transposition type, there are many DORV variants that have neither aortomitral nor pulmonary-mitral continuity and have variable distribution of the conal septum.

The length of conus determines the location of VSD relative to the tricuspid valve and semilunar valve with a longer conus increasing the distance between the VSD and semilunar valves.[10]

Routability

A highly important surgical determinant is the routablity of the VSD (Supplemental Video 1, Supplemental Digital Content 1, http://links.lww.com/JTI/A115). The location of the VSD, as determined from the RV side (repair is performed from the RV side), depends on its relationship to the semilunar valve and the orientation of the outlet septum. If the outlet septum is fused to the left margin of the VSD, it is subaortic (Fig. 4, Supplemental Video 2, Supplemental Digital Content 2, http://links.lww.com/JTI/A116 virtual model subaortic VSD), and, if the outlet septum is fused to the right margin of the VSD, it is subpulmonary (Fig. 5, Supplemental Video 3, Supplemental Digital Content 3, http://links.lww.com/JTI/A117, virtual model subpulmonary VSD). If the distance between the VSD and the semilunar valves is more than the size of the aortic valve, it is termed as noncommitted VSD (Fig. 6, virtual model with remote VSD). However, even in patients with long conal length, the VSD may appear remote. In such patients, alignment of the VSD to either

outflow tract should be mentioned. In doubly committed VSD, it is related to both valves with the absence of the infundibulum (Fig. 6).[11] Virtual 3-dimensional models could be created (www.slicer.org) and displayed using virtual reality headsets to simulate real-time interaction with heart models (Supplemental Video 4, Supplemental Digital Content 4, http://links.lww.com/JTI/A118, Video 5, Supplemental Digital Content 5, http://links.lww.com/JTI/A119). These can be utilized both for surgical planning and educational purposes.

The location of the VSD in relation to tricuspid annulus is also important, as, during intraventricular baffling, there may be tricuspid valve damage (if VSD abuts tricuspid valve septal leaflet) (Fig. 4).[12]

In subaortic VSD, repair is carried out by creating an intraventricular tunnel using a Gore-Tex patch as a baffle to divert blood from the VSD to the aorta (Fig. 7). Arterial switch operation with creation of aorta to ventricular tunnel is preferred in subpulmonary VSD with right ventricular outflow obstruction (Supplemental Video 6, Supplemental Digital Content 6, http://links.lww.com/JTI/A120, Supplemental Video 7, Supplemental Digital Content 7, http://links.lww.com/JTI/A121).

Doubly committed VSD also involves tunnel repair, whereas noncommitted VSD requires complex biventricular repair if the ventricles are of an adequate size.[13] Intraventricular baffling is possible in patients with remote septal defect if VSD aligns with either outflow tract.

Other Associated Anomalies With Surgical Considerations

Sizing of Ventricles

Adequate size of ventricles and atrioventricular valves determine whether biventricular repair can be undertaken in such patients. Adequate right ventricular volume should be present for intraventricular baffling, and this can be measured preoperatively if retrospective CT (scan throughout the cardiac cycle with ECG-gated dose modulation to save radiation

FIGURE 13. Associated coronary arterial anomalies. A, Axial CT angiography (CTA) image displays separate origin of the left circumflex and left anterior descending coronary artery from the left aortic sinus. B, Reformatted coronal CTA image shows dilated right coronary artery. C, Axial CTA image shows origin of all coronaries from the same anterior aortic sinus. D, Axial CTA image shows origin of the left anterior descending coronary from the right coronary artery. LAD indicates left anterior descending coronary artery; LCX, left circumflex coronary artery; RCA, right coronary artery.

dose) is performed. In patients with tricuspid or mitral atresia, if ventricular size is small, staged palliative repair—as for single-ventricle physiology—is performed (Fig. 8).[14] There are no uniformly applicable numeric criteria for univentricular versus biventricular repair in a hypoplastic LV. However, in patients with critical aortic stenosis, it has been postulated that indexed left ventricular end-diastolic volume <20 mL/m2 has poor prognostic value.[15]

Aortic Anomalies

Aortic anomalies or variations that can be encountered include a right-sided aortic arch, presence of aberrant subclavian artery, anomalous origin of pulmonary artery from the ascending aorta, bovine arch, patent ductus arteriosus, arch hypoplasia, and coarctation of aorta (Fig. 9). In the subgroup of patients with left ventricular outflow obstruction such as arch hypoplasia, the VSD to pulmonary artery baffle can be created during repair.[16]

Pulmonary Arterial Anomalies

Commonly associated pulmonary arterial anomalies include infundibular PS, supravalvular PS, and/or atresia of pulmonary arteries (Fig. 10). During intraventricular repair,

FIGURE 14. Miscellaneous associations. A, Axial CT angiography (CTA) image shows juxtaposed atrial appendages: right atrial and finger-like left atrial appendages are both lying on the same (left) side. B, Axial CTA image in a different patient shows balanced common atrioventricular canal defect. C, Axial CTA image in another patient with unbalanced common atrioventricular canal defect. D and E, Reformatted coronal and axial CTA images with ectopia cordis: the heart is lying in the abdominal cavity (below diaphragm) with midline abdominal wall defect. CAVC indicates common atrioventricular canal defect; LAA, left atrial appendage; RAA, right atrial appendage.

PS can be repaired either by resection of the septum or by using a conduit or a patch.[16]

Anomalous Systemic and Pulmonary Venous Drainage

Associated venous drainage anomalies include persistent left superior vena cava, retroaortic left brachiocephalic vein, and partial (PAPVC) and total anomalous pulmonary venous drainage (TAPVC) (Figs. 11, 12). PAPVC and TAPVC are commonly seen in the right and left atrial isomerism, respectively.[17,18] Presurgical knowledge of systemic venous anomalies is important, as it holds significance in the institution of cardiopulmonary bypass and venous cannulations.

Coronary Arterial Anomalies

Coronary artery anomalies include the separate origin of the left circumflex and left anterior descending coronary artery, dilated right coronary artery, origin of left anterior descending from right coronary artery, and origin of all coronary arteries from the same aortic sinus (Fig. 13, Supplemental Video 8, Supplemental Digital Content 8, http://links.lww.com/JTI/A122). Unidentified coronary anomalies can result in disastrous surgical outcomes including mortality.

Miscellaneous Associations

DORV may also be associated with juxtaposed atrial appendages,[12] atrial septal defect, and balanced and unbalanced (Supplemental Video 9, Supplemental Digital Content 9, http://links.lww.com/JTI/A123) atrioventricular canal defects, and incidental findings like left atrial appendage thrombus can also be encountered. Noncardiac anomalies may include right congenital diaphragmatic hernia[19] and bronchogenic cysts. Extremely rare cardiac defects to be seen include Pentalogy of Cantrell with ectopia cordis and midline supraumbilical defect (Fig. 14).

Role of CT Angiography in Postoperative Imaging

Although, nowadays, MRI is routinely used in the postoperative imaging of DORV patients, it has its inherent disadvantages, as discussed above.[2,7] CT is a reliable substitute in this scenario, especially in the developing and underdeveloped countries, because of its widespread availability and relatively lower cost. It is used in the assessment of both palliative and surgical repairs like Blalock-Taussig shunt, bidirectional Glenn shunt, total cavopulmonary connection, and Fontan circulation (Fig. 15). It can identify complications secondary to the surgical procedure like stenosis or blockage of these shunts.[7] Functional assessment is also possible in desired cases for which a retrospective ECG gated scan may be performed, and images reconstructed in the different phases of the cardiac cycle to get a detailed volumetric analysis.

CONCLUSIONS

Noninvasive multiplanar and multidimensional CT imaging is invaluable in both the preoperative and postoperative

FIGURE 15. Postoperative imaging in patients of double-outlet right ventricle. A, Multiplanar coronal reformatted CT angiography (CTA) image with Blalock-Taussig shunt: a graft is connecting the left subclavian artery to the left pulmonary artery. B, Coronal reformatted CTA image shows total cavopulmonary connection (both superior and inferior vena cava connected to the pulmonary artery) with presence of patent left pulmonary artery stent (arrow). C, Reformatted coronal CTA image shows right bidirectional Glenn (BDG) shunt: the right superior vena cava is connected to the pulmonary artery via a graft. D, Coronal reformatted CTA image shows a thrombus in the inferior vena cava (Blocked fontan shunt). BT indicates Blalock-Taussig; IVC, inferior vena cava; LPA, left pulmonary artery; SCA, subclavian artery; SVC, superior vena cava.

assessment of patients with DORV. Dual-source CT scanners have a high spatial and temporal resolution and utilize low-dose modulation techniques that limit the radiation dose. Because of the widespread availability of CT, as compared with MRI, especially in the low-income group countries, the use of current-generation CT scanners utilizing low-dose technology seems a well-suited choice in the imaging evaluation of DORV.

REFERENCES

1. Vitiello R, McCrindle BW, Nykanen D, et al. Complications associated with pediatric cardiac catheterization. *J Am Coll Cardiol*. 1998;32:1433–1440.
2. Tangcharoen T, Bell A, Hegde S, et al. Detection of coronary artery anomalies in infants and young children with congenital heart disease by using MR imaging. *Radiology*. 2011;259:240–247.

3. Shi K, Yang ZG, Chen J, et al. Assessment of double outlet right ventricle associated with multiple malformations in pediatric patients using retrospective ECG-gated dual-source computed tomography. *PLoS One*. 2015;10:e0130987.

4. Lacour-Gayet F. Intracardiac repair of double outlet right ventricle. *Semin Thorac Cardiovasc Surg Pediatr Card Surg Annu*. 2008;11: 39–43.

5. Chen SJ, Li YW, Wang JK, et al. Three-dimensional reconstruction of abnormal ventriculoarterial relationship by electron beam CT. *J Comp Assist Tomo*. 1998;22:560–568.

6. Freedon R, Smallhorn J. Double outlet right ventricle. In: Freedon R, Benson L, Smallhorn J, eds. *Neonatal Heart Disease*, 1st ed. London: Springer Verlag; 1992:453–470.

7. Frank L, Dillman JR, Parish V, et al. Cardiovascular MR imaging of conotruncal anomalies. *Radiographics*. 2010;30:1069–1094.

8. Sondheimer HM, Freedom RM, Olley PM. Double outlet right ventricle: clinical spectrum and prognosis. *Am J Cardiol*. 1977;39: 709–714.

9. Howell CE, Ho SY, Anderson RH, et al. Fibrous skeleton and ventricular outflow tracts in double-outlet right ventricle. *Ann Thorac Surg*. 1991;51:394–400.

10. Anderson RH, McCarthy K, Cook AC. Double outlet right ventricle. *Cardiol Young*. 2001;11:329–344.

11. Walters HL III, Mavroudis C, Tchervenkov CI, et al. Congenital Heart Surgery Nomenclature and Database Project: double outlet right ventricle. *Ann Thorac Surg*. 2000;69(suppl 4):S249–S263.

12. Yim D, Dragulescu A, Ide H, et al. Essential modifiers of double outlet right ventricle: revisit with endocardial surface images and 3-dimensional print models. *Circ Cardiovasc Imaging*. 2018;11:e006891.

13. Cetta F, Boston US, Dearani JA, et al. Double outlet right ventricle: opinions regarding management. *Curr Treat Options Cardiovasc Med*. 2005;7:385–390.

14. Russo P, Danielson GK, Puga FJ, et al. Modified Fontan procedure for biventricular hearts with complex forms of double-outlet right ventricle. *Circulation*. 1988;78(pt 2): III20–III25.

15. Hammon JW Jr, Lupinetti FM, Maples MD, et al. Predictors of operative mortality in critical valvular aortic stenosis presenting in infancy. *Ann Thorac Surg*. 1988;45:537–540.

16. Brown JW, Ruzmetov M, Okada Y, et al. Surgical results in patients with double outlet right ventricle: a 20-year experience. *Ann Thorac Surg*. 2001;72:1630–1635.

17. Ghosh S, Yarmish G, Godelman A, et al. Anomalies of visceroatrial situs. *AJR Am J Roentgenol*. 2009;193:1107–1117.

18. Lapierre C, Déry J, Guérin R, et al. Segmental approach to imaging of congenital heart disease. *Radiographics*. 2010;30: 397–411.

19. Lin AE, Pober BR, Adatia I. Congenital diaphragmatic hernia and associated cardiovascular malformations: type, frequency, and impact on management. *Am J Med Genet C Semin Med Genet*. 2007;145C:201–216.